



## Beyond the Coherent Coupled Channels Description of Nuclear Fusion

M. Dasgupta,<sup>1</sup> D. J. Hinde,<sup>1</sup> A. Diaz-Torres,<sup>1</sup> B. Bouriquet,<sup>1,\*</sup> Catherine I. Low,<sup>1,†</sup> G. J. Milburn,<sup>2</sup> and J. O. Newton<sup>1</sup>

<sup>1</sup>*Department of Nuclear Physics, Research School of Physical Sciences and Engineering, Australian National University, Canberra, ACT 0200, Australia*

<sup>2</sup>*Department of Physics, University of Queensland, St. Lucia, QLD 4072, Australia*

(Received 8 June 2007; published 6 November 2007)

New measurements of fusion cross sections at deep sub-barrier energies for the reactions  $^{16}\text{O} + ^{204,208}\text{Pb}$  show a steep but almost saturated logarithmic slope, unlike  $^{64}\text{Ni}$ -induced reactions. Coupled channels calculations cannot simultaneously reproduce these new data and above-barrier cross-sections with the same Woods-Saxon nuclear potential. It is argued that this highlights an inadequacy of the coherent coupled channels approach. It is proposed that a new approach explicitly including gradual decoherence is needed to allow a consistent description of nuclear fusion.

DOI: [10.1103/PhysRevLett.99.192701](https://doi.org/10.1103/PhysRevLett.99.192701)

PACS numbers: 25.70.Jj, 03.65.Yz, 24.10.Eq

Nuclear fusion involves a massive rearrangement of a complex quantum system with many degrees of freedom. For simplicity, the nuclear interactions are represented by a short-range attractive nuclear potential, which combined with the long-range repulsive Coulomb potential forms a barrier against fusion. In the simplest barrier-passing model, if the barrier is overcome, fusion occurs. The failure to describe sub-barrier fusion of heavy nuclei [1,2] demonstrated the need to include the effects of internal nuclear degrees of freedom explicitly [3]. The coupled channels model, including collective couplings, successfully explained precise fusion cross sections at near-barrier energies [4].

The nuclear potential, a key ingredient in these calculations, is a construct to account for the many-body interactions between the protons and neutrons in the two nuclei that are not explicitly included through channel couplings. Commonly a Woods-Saxon (W-S) form is used:  $V_n(r) = V_0[1 + \exp\{(r - R)/a\}]^{-1}$ , where  $V_0$ ,  $R$ , and  $a$  are the depth, radius, and the diffuseness parameters, respectively. Since the Coulomb interaction is known exactly, the parameters of  $V_n$  determine the fusion barrier energy, the internuclear separation ( $r$ ) at the top of the barrier (the barrier radius), and the barrier width. The parameters may be constrained by requiring that the calculations are consistent with fusion measurements [5]. They may also be taken from systematic parameterizations [6] of fits to scattering data. The latter give diffuseness parameters typically between 0.6 and 0.8 fm, in agreement with calculations of the semi-microscopic double-folding model [7]. However, these parameters systematically predict much higher fusion cross sections above the barrier than those measured [8]. Only by using diffuseness parameters up to twice those expected can the experimental fusion data be reproduced [8]. Recent measurements of fusion at energies far below the fusion barrier [9] have brought to light another problem: cross sections fall much more rapidly than coupled channels predictions using standard nuclear potentials. A very shallow nuclear potential has been proposed [10,11]

to explain these measurements. However, as discussed later, at energies well above the barrier, this approach presents a significant logical problem, as the potential pocket disappears at higher angular momenta.

We present new experimental measurements of fusion cross sections at deep sub-barrier energies for the reactions  $^{16}\text{O} + ^{204,208}\text{Pb}$ , complementing existing above-barrier measurements [12,13]. Together they show that the coherent coupled channels approach is inadequate to describe fusion. It is argued that this approach is unrealistic as it implicitly assumes that energy dissipation (irreversibility) sets in at some point inside the barrier without affecting quantum coherence. It is proposed that a model with a gradual onset of decoherence between the superposed states is necessary to provide a realistic solution to the problems of modelling nuclear fusion.

Pulsed beams ( $\approx 1$  ns wide) of  $^{16}\text{O}$  in the energy range 74.0–102.0 MeV, provided by the ANU 14UD electrostatic accelerator, bombarded  $>99\%$  enriched targets of  $^{208}\text{PbS}$  and  $^{204}\text{PbS}$ , of  $\sim 90 \mu\text{g}/\text{cm}^2$  thickness, evaporated onto  $20 \mu\text{g}/\text{cm}^2$  C backings. The stability of the monitor energy spectra and count rates showed that target degradation was successfully minimized by limiting the beam current and translating the targets. The compound nuclei formed following fusion decay mainly by fission, only a small fraction resulting in evaporation residues.

Fission fragments were measured in coincidence using two large position sensitive multiwire proportional counters [14]. Energy loss and kinematical coincidence requirements resulted in essentially no background events even at the lowest energy. Recoiling evaporation residues (ERs) were separated by a compact velocity filter [15] and implanted into a silicon detector, where they were uniquely identified by their  $\alpha$ -decay energies. Normalization of both measurements used Rutherford scattering.

Heavy target impurities were determined at ppb levels using laser-ablation inductively-coupled plasma mass spectrometry [16]. Those in  $^{208}\text{Pb}$  were below ppm levels, while 54 ppm of tungsten was found for  $^{204}\text{Pb}$ . Corrections

were made by measuring fission from targets of the contaminant elements. These were significant only at the lowest energy for  $^{204}\text{Pb}$ , the correction of 14% being consistent with the kinematically determined mean center-of-mass (c.m.) velocity associated with fission.

The fission cross sections ( $\sigma_{\text{fis}}$ ) were measured down to c.m. energies ( $E$ ) of 66 and 67 MeV, respectively, for  $^{208}\text{Pb}$  and  $^{204}\text{Pb}$ , where  $\sigma_{\text{fis}} \sim 10^{-5}$  mb. Because of the lower efficiency, the ER cross sections ( $\sigma_{\text{ER}}$ ) for  $^{208}\text{Pb}$  were only measured down to 69 MeV, where  $\sigma_{\text{ER}}$  is a few  $10^{-3}$  mb. At lower energies, they were estimated by extrapolating the measured  $\sigma_{\text{ER}}/\sigma_{\text{fis}}$ , which varies slowly with energy (Fig. 1). The thin full lines are exponential fits, while the thick line is a modulation to the fit to the  $^{208}\text{Pb}$  data that reproduces the discrete nature of the competition between fission and neutron evaporation. This was used to extrapolate to the lowest energies for this reaction (dashed line). For the  $^{204}\text{Pb}$  reaction,  $\sigma_{\text{ER}}/\sigma_{\text{fis}}$  is smaller, and in both reactions, varying the extrapolations by 50% does not change the conclusions, as fission is the dominant decay mode. The fusion cross sections ( $\sigma = \sigma_{\text{fis}} + \sigma_{\text{ER}}$ ) are shown in Fig. 2, together with the results of previous measurements [12,13] at higher energies. The two reactions are in excellent agreement.

The energy regions of interest here are well below and well above the barrier. At the lower energies, taking the logarithmic slope  $d[\ln(E\sigma)]/dE$  [9] allows comparison of the tunnelling gradient independent of the weight of the lowest barrier (Fig. 3), while at above-barrier energies, data are shown on a linear scale [Fig. 4(a)]. Neither the logarithmic slope at below-barrier energies, nor the energy dependence of the cross sections well above the barrier depend on couplings. Nevertheless, comparisons are initially made with coupled channels calculations to demonstrate that the observed deviations are not due to neglect of couplings.

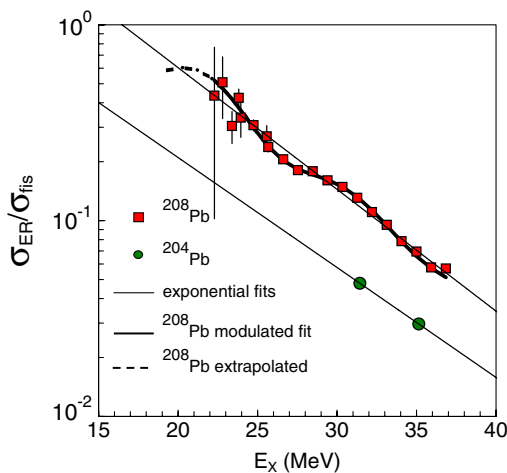


FIG. 1 (color online). Ratio of evaporation residue to fission cross sections as a function of excitation energy of the compound nucleus. The lines are fits to the data (see text).

The calculations used the code CCFULL [17], with an ingoing wave boundary condition applied at the bottom of the ( $\ell$ -dependent) potential pocket. The W-S nuclear potential depth and radius were chosen to match the calculated average barrier energy to experiment. Initial calculations used a diffuseness  $a = 0.66$  fm, consistent with double-folding model calculations and the W-S parametrization of the Aküz-Winther potential [6]. Couplings to the collective  $3^-$ ,  $5^-$ , and double octupole phonon states (in the harmonic limit) in  $^{208}\text{Pb}$  were included [12].

The calculations (dashed line in Fig. 3) do not match the initial rise of the experimental slope, indicating that the energy of the lowest barrier is not exactly reproduced. This is not unexpected in view of the limited understanding of the couplings (particularly transfer) affecting fusion. Shifting the calculations down in energy by 0.8 MeV (thin full line) gives a good match to the rising part of the logarithmic slope. The “saturation” slope at low  $E$  is hardly affected by this shift, or even by neglecting couplings entirely (thick full line). Thus, at deep sub-barrier energies, measurements can be compared with coupled channels calculations, shifted calculations, or no-coupling calculations without affecting the conclusions. At these energies, the measured slope lies well above those calculated, but does show clear evidence of saturation, which is significantly different from the reaction  $^{64}\text{Ni} + ^{64}\text{Ni}$  [9], where the slope keeps increasing with decreasing energy.

These calculations also fail to reproduce measured cross sections at energies well above the barrier, predicting much higher values, as shown in Fig. 4(a). Constraining the average barriers to match experiment, calculations with couplings (thin line) and without (short dashed line) are almost identical, showing that the disagreement is independent of couplings. The above-barrier data can be reproduced using a larger value of the diffuseness parameter, as

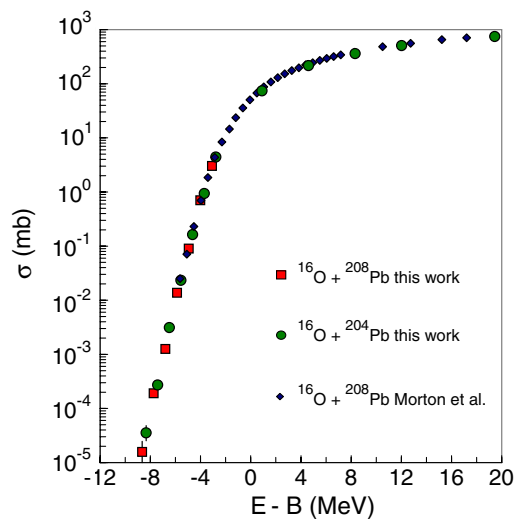


FIG. 2 (color online). Fusion cross sections as a function of the center-of-mass energy with respect to the barrier energies  $B = 74.5$  and  $74.9$  MeV for  $^{208}\text{Pb}$  and  $^{204}\text{Pb}$ , respectively.

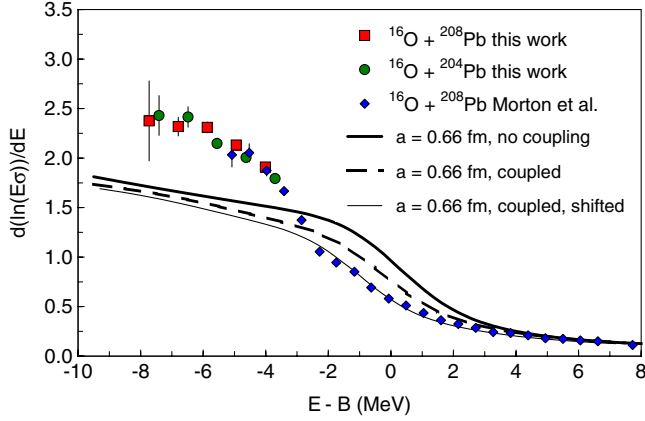


FIG. 3 (color online). Logarithmic slope as a function of energy with respect to the barrier. Calculation with standard parameters fail to match the measurements at low energy.

found in earlier works; a diffuseness  $a = 1.18$  fm (with  $V_0 = 300$  MeV) gives good agreement [dashed line in Fig. 4(a)]. Using this diffuseness [dashed line in Fig. 4(b)], the measured logarithmic slope at deep sub-barrier energies is not reproduced, for which a diffuseness parameter of 1.65 fm is required, as shown by the thick line. Figure 4(a) shows that this completely fails to reproduce the above-barrier cross sections.

The failure to obtain a simultaneous description of below- and above-barrier fusion data, which are essentially

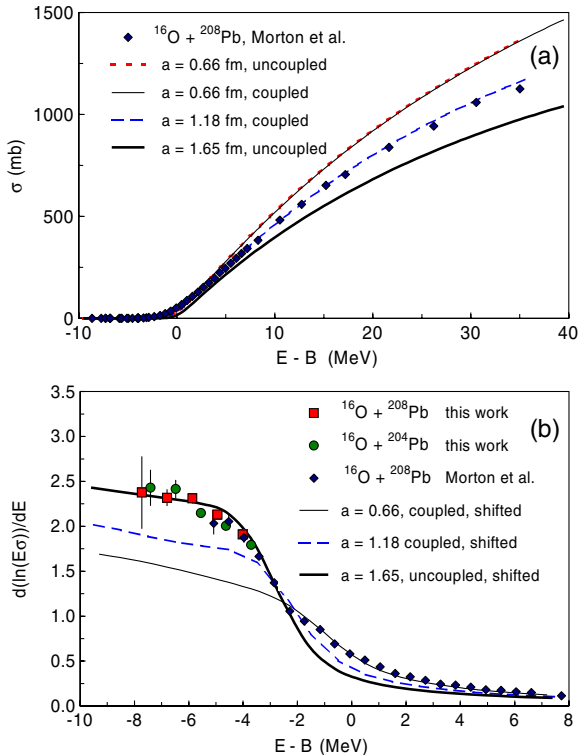


FIG. 4 (color online). Calculations which reproduce  $\sigma$  above the barrier (a) fail to reproduce the low energy data (b).

unaffected by couplings, might be due to physical effects not included. How could these affect both deep sub-barrier and above-barrier fusion? At deep sub-barrier energies,  $d[\ln(E\sigma)]/dE$  is dependent on the barrier width, characterized by the outer and inner turning points. At a given above-barrier energy, the cross section is determined by the limiting angular momentum ( $\ell\hbar$ ) that results in fusion. In the model, this is determined by the corresponding high- $\ell$  barrier energy and radius, which occurs at a smaller inter-nuclear separation than the  $\ell = 0$  barrier. Thus, the inner turning point for a given energy below the barrier is at the *same* separation as the top of the fusion barrier for the limiting angular momentum at a corresponding above-barrier energy [18]. This is true independent of the particular form of the nuclear potential (expected to be energy-independent over the 20–50 MeV energy range relevant here).

It follows that any *physical* mechanism invoked to reproduce the below-barrier measurements should also reproduce those above-barrier (and vice versa). This has not been true of explanations put forth thus far. A shallow nuclear potential, which at small separations deviates from the Woods-Saxon form, has been proposed to explain deep sub-barrier fusion data [11]. This may be part of the explanation, but cannot be the complete picture, as a shallow potential leads to no trapping potential pocket for higher angular momenta. Here, fusion only occurs by the application of an ingoing wave boundary condition at a fixed radius [11]. However, this implies energy damping processes at that radius which should also affect tunnelling probabilities below the barrier. The use of large diffuseness values as empirical fit parameters for above-barrier data [5,12] are not satisfactory either, as they fail to simultaneously describe deep sub-barrier fusion data.

In the coherent coupled channels model, the total wave function is written as a linear superposition of a (limited) number of basis states, which is subject to Hamiltonian unitary evolution. Capture, which in reality occurs through an irreversible loss of translational kinetic energy to the multitude of single particle degrees of freedom, is simulated by applying an ingoing wave boundary condition or a short-ranged imaginary potential. Although the model implicitly (and correctly) includes irreversibility at some distance inside the barrier, the significant implication of irreversibility on the coherent superposition is neglected. Irreversibility cannot occur without decoherence, which rapidly transforms the linear superposition of state vectors into a mixed state described by a density matrix ( $\rho$ ):

$$\begin{aligned} |\psi\rangle &= \alpha|\psi_1\rangle + \beta|\psi_2\rangle \Rightarrow \rho \\ &= |\alpha|^2|\psi_1\rangle\langle\psi_1| + |\beta|^2|\psi_2\rangle\langle\psi_2|. \end{aligned}$$

Decoherence is fundamental to open quantum systems, and results from the interaction between the explicitly included degrees of freedom and other (typically many) degrees of freedom, called the environment [19,20]. Increasing the

size of the basis in the coherent coupled channels approach (to include states identified with the environment) will not result in decoherence. Decoherence can be modeled in an explicitly time-dependent density matrix approach. The effects of decoherence in condensed matter physics and quantum optics are now well recognized [19–21]. Decoherence is often, but not always, associated with energy dissipation. It was demonstrated that dissipation decreases quantum tunnelling in the pioneering work of Ref. [22], where the environment was modeled as a large number of harmonic oscillators. In other systems, the environment is identified as the quasi continuum of states coupled to the quasibound states of an unstable system, describing, for example, the decay of an optical cavity mode in quantum optics [23].

In nuclear fusion, the environment cannot be external to the two colliding nuclei. However, it is clear that the environmental degrees of freedom must fall outside the coupled channels model space, which describes an entirely coherent quantum system. Identifying the environment with internal nucleonic degrees of freedom implies that couplings to the environment should have a strong radial dependence; this coupling could be direct or through doorway states such as the giant resonances [24]. This immediately suggests that the environment acts as an effective position measurement of the radial coordinate. It gives a mechanism by which the resulting decoherence can change tunnelling rates, as demonstrated experimentally in atom optics [25], where the decay of a quasibound cold atom can be changed due to repeated observations of its position.

A gradual onset of decoherence [21] with increasing nuclear overlap may be thought of as making the system gradually more classical. In fusion, as beam energies are reduced further below the barrier, decoherence should increasingly suppress the sub-barrier fusion enhancement that results from the coherent superposition. It can also result in energy dissipation, giving angular momentum and energy loss for higher partial waves, which will change the above-barrier fusion cross sections.

This suggested approach differs from dynamical models up to now, which have either been formulated in the extreme limits of a completely coherent quantum picture where no energy dissipation can occur, or have included dissipation classically, semiclassically, or using statistical concepts. To our knowledge, there is no quantum dynamical model of nuclear reactions that explicitly includes decoherence, although first steps in this direction have been taken using the Lindblad equation [26]. Such a model would naturally include system-environment couplings, and provide an avenue to reconcile the coherent coupled channels model with classical models of energy dissipation which describe deep-inelastic scattering. It may also have significant implications for astrophysical (very low energy)

fusion reactions, where the inner turning point is far inside the barrier.

We thank K. Hagino and J. A. Tostevin for illuminating discussions, C. M. Allan for assisting with target composition measurements, C. R. Morton and A. C. Berriman for assistance during initial ER measurements, and R. A. Yanez in the fission measurements. M.D. and D.J.H. acknowledge the support of an ARC Discovery Grant.

---

\*Current address: C.E.R.F.A.C.S., 31057 Cedex 01, France.

†Current address: Rangī Ruru Girls' School, Christchurch, New Zealand.

- [1] R. G. Stokstad *et al.*, Phys. Rev. C **21**, 2427 (1980).
- [2] A. B. Balantekin *et al.*, Phys. Rev. C **28**, 1565 (1983).
- [3] C. H. Dasso *et al.*, Nucl. Phys. A **405**, 381 (1983); **407**, 221 (1983).
- [4] M. Dasgupta *et al.*, Annu. Rev. Nucl. Part. Sci. **48**, 401 (1998).
- [5] J. R. Leigh *et al.*, Phys. Rev. C **52**, 3151 (1995).
- [6] R. A. Broglia and A. Winther, *Heavy Ion Reactions* (Benjamin/Cummings, Reading, Massachusetts, 1981), Vol. I.
- [7] I. I. Gontchar *et al.*, Phys. Rev. C **69**, 024610 (2004).
- [8] J. O. Newton *et al.*, Phys. Lett. B **586**, 219 (2004); Phys. Rev. C **70**, 024605 (2004).
- [9] C. L. Jiang *et al.*, Phys. Rev. Lett. **93**, 012701 (2004).
- [10] C. H. Dasso and G. Pollarolo, Phys. Rev. C **68**, 054604 (2003).
- [11] Ş. Mişicu and H. Esbensen, Phys. Rev. Lett. **96**, 112701 (2006).
- [12] C. R. Morton *et al.*, Phys. Rev. C **60**, 044608 (1999).
- [13] D. J. Hinde *et al.*, Phys. Rev. Lett. **89**, 282701 (2002).
- [14] D. J. Hinde *et al.*, Phys. Rev. C **53**, 1290 (1996).
- [15] J. X. Wei *et al.*, Nucl. Instrum. Methods Phys. Res., Sect. A **306**, 557 (1991).
- [16] G. F. Durrant, Journal of Analytical Atomic Spectrometry **14**, 1385 (1999).
- [17] K. Hagino, N. Rowley, and A. T. Kruppa, Comput. Phys. Commun. **123**, 143 (1999).
- [18] M. Dasgupta *et al.*, *FUSION06*, AIP Conf. Proc. 853, 21 (2006).
- [19] C. Kiefer and Erich Joos, *Quantum Future: Proceedings of the Xth Max Born Symposium* (Springer-Verlag, Berlin, 1999), p. 105.
- [20] M. Schlosshauer, *Decoherence and the Quantum-to-Classical Transition* (Springer-Verlag, Berlin, 2007).
- [21] P. Sonnentag and F. Hasselbach, Phys. Rev. Lett. **98**, 200402 (2007).
- [22] A. O. Caldeira and A. J. Leggett, Phys. Rev. Lett. **46**, 211 (1981).
- [23] G. J. Milburn and D. F. Walls, *Quantum Optics* (Springer, Berlin, 1994), Chap. 16.
- [24] R. A. Broglia *et al.*, Phys. Lett. B **61**, 113 (1976).
- [25] M. C. Fischer, B. Gutierrez-Medina, and M. G. Raizen, Phys. Rev. Lett. **87**, 040402 (2001).
- [26] M. Genkin and W. Scheid, J. Phys. G **34**, 441 (2007).